Elsevier Editorial System(tm) for Journal of Sound and Vibration

Manuscript Draft

Manuscript Number: JSV-D-20-00903R3

Title: A Hybrid Finite Element-Statistical Energy Analysis Approach to the Dynamic Response of Built-up Systems with Nonlinear Joints

Article Type: Full Length Article

Section/Category: I Nonlinear aspects of sound and vibration

Keywords: Nonlinear analysis; Statistical energy analysis; Lagrange-Rayleigh-Ritz formulation; Method of harmonic balance; Dynamic systems.

Corresponding Author: Dr. Fiorenzo A. Fazzolari, Ph.D.

Corresponding Author's Institution: University of Liverpool

First Author: Fiorenzo A. Fazzolari, Ph.D.

Order of Authors: Fiorenzo A. Fazzolari, Ph.D.; Puxue Tan

Abstract: The present article deals with the development and validation of a hybrid finite element-statistical energy analysis (FE-SEA) formulation employed to obtain the ensemble-average of the time-averaged vibrational energy response of dynamic systems with nonlinear joints. The proposed FE-SEA formulation is validated via a nonlinear stochastic benchmark model. The theoretical formulation related to the latter, is entirely derived by employing a variational approach. The weak-form of the governing equations, for each of the sample in the ensemble, is based on Kirchhoff's thin-plate assumptions and is restricted to the out-of-plane motion only. The classical Lagrange-Rayleigh-Ritz method (LRRM), combined with the Monte Carlo simulation (MCS), is used as solution technique. An appropriate degree of uncertainty is introduced into the model in order to break the system symmetries ensuring transition from an exponential to a Rayleigh distribution of the modal spacing. Both in the hybrid FE-SEA and in the LRRM+MCS the localised nonlinearities are linearised by means of the method of harmonic balance. Various built-up plate systems, consisting of rectangular isotropic, homogeneous and linear elastic plates, elastically coupled by virtue of nonlinear translational and/or torsional springs and subjected to harmonic point loads are investigated.

Delft University of Technology
Faculty of Civil Engineering and Geosciences,
Stevinweg 1, 2600 GA, Delft,
Netherlands

August 7, 2020

Dear Prof. A. V. Metrikine,

A Hybrid Finite Element-Statistical Energy Analysis Approach to the Dynamic Response of Built-up Systems with Nonlinear Joints

The paper has been modified according to the reviewers suggestions. We do hope the present version of the manuscript is suitable for publication in the *Journal of Sound and Vibration*.

Looking forward to hearing from you in due course.

With kind regards,

Fiorenzo A. Fazzolari

Highlights

- A hybrid FE-SEA formulation accounting for nonlinearities has been developed.
- The employed randomisation process led to the GOE statistics efficiently.
- A nonlinear stochastic benchmark model based on the MCS has been used.
- The hybrid FE-SEA showed a high level of accuracy with low computational cost.
- The MHB turned out to be an effective and efficient technique for the linearisation.

A Hybrid Finite Element-Statistical Energy Analysis Approach to the Dynamic Response of Built-up Systems with Nonlinear Joints

Fiorenzo A. Fazzolari[1,*], Puxue Tan[1]

University of Liverpool, School of Engineering, Brownlow Hill, Liverpool, L69 3GH, UK

Abstract

The present article deals with the development and validation of a hybrid finite element-statistical energy analysis (FE-SEA) formulation employed to obtain the ensemble-average of the time-averaged vibrational energy response of dynamic systems with nonlinear joints. The proposed FE-SEA formulation is validated via a nonlinear stochastic benchmark model. The theoretical formulation related to the latter, is entirely derived by employing a variational approach. The weak-form of the governing equations, for each of the sample in the ensemble, is based on Kirchhoff's thin-plate assumptions and is restricted to the out-of-plane motion only. The classical Lagrange-Rayleigh-Ritz method (LRRM), combined with the Monte Carlo simulation (MCS), is used as solution technique. An appropriate degree of uncertainty is introduced into the model in order to break the system symmetries ensuring transition from an exponential to a Rayleigh distribution of the modal spacing. Both in the hybrid FE-SEA and in the LRRM+MCS the localised nonlinearities are linearised by means of the method of harmonic balance. Various built-up plate systems, consisting of rectangular isotropic, homogeneous and linear elastic plates, elastically coupled by virtue of nonlinear translational and/or torsional springs and subjected to harmonic point loads are investigated.

Keywords: Nonlinear analysis, Statistical energy analysis, Lagrange-Rayleigh-Ritz formulation, Method of harmonic balance, Dynamic systems.

1. Introduction

Manufacturing and material imperfections, which affect significantly the prediction of the system response, widely exist in the engineering structures. The dynamic response of sys-

*Corresponding author: Fiorenzo Fazzolari, Tel:+44 (0)151 794 5227
Email address: Fiorenzo.Fazzolari@liverpool.ac.uk (Fiorenzo A. Fazzolari)
[1]Department of Mechanical, Materials and Aerospace Engineering

tems at both mid- and high-frequency range is highly sensitive to the structural uncertainties. Therefore, computational methods for the structural analysis accounting for uncertainties are required. In order to overcome these shortcomings, the statistical energy analysis (SEA) was introduced. The SEA aims to model the average vibrational energy flow between an arbitrary number of subsystems which are generally part of a complex structures. It also utilizes loss factor to represent energy dissipation in subsystems, and coupling loss factor (CLF) is employed in order to describe the dynamic interaction between subsystems. It has been extensively researched over the last decades, and it turned out to be an extremely powerful tool when analysing the dynamic behaviour of structures subjected to externally imposed vibration sources acting from the mid- to high-frequency range. The traditional SEA has been comprehensively discussed by Lyon [1], who via algebraic equations related the average energy stored and dissipated in subsystems to the energy input from the external sources or other subsystems. A comprehensive overview of the topic has been provided by Fahy [2] and Woodhouse and Hodges [3]. The authors provided physical insights on the SEA and discussed different approaches that can be used to solve the main problem of the SEA. Langley [4, 5] derived a general form of the SEA equations and the CLF aiming to analyse the response of multi-coupled systems under the condition of weak coupling. However, the classical SEA is essentially limited to the high-frequency range. As regards the low-frequency range classical deterministic methodologies such as finite element (FE) method can be successfully used. Problems occur when dealing with the mid-frequency range where SEA is not applicable as the system is not featured by enough uncertainties, while FE is computationally expensive [6]. In order to overcome this drawback, Langley and Shorter derived a ground-breaking formulation referred to as hybrid finite element-statistical energy analysis (FE-SEA) formulation [7, 8]. This approach allows to properly determine the response of highly complex dynamic systems with no loss of accuracy in the mid-frequency range. In this specific range the deterministic components of the system are small if commensurate to a wavelength, then prone to be modelled using FE, while some others are large when compared with a wavelength, thus amenable to be treated statistically by SEA. The statistical concepts and methods which lie behind the SEA are based on the Gaussian Orthogonal Ensemble (GOE). With respect to the originally adopted Poisson process, mainly used for convenience, and based on the assumption that the system is featured by many symmetries, the GOE statistics turned out to provide a more realistic description. One important characteristic is that when uncertainty

applies, the distribution of spacings of natural frequency is of Rayleigh-type not exponential, which conforms to GOE statistics [9]. Based on this assumption the average vibrational energy flow is determined, however, a second quantity which is of noteworthy interest is the variance. Lyon [10] has derived the variance by using probability density function (pdf) of modal spacings. Langley and Cotoni [11, 12] have given a variance prediction method for general built-up structures along with its simulation and experimental validation. With respect to the hybrid FE-SEA model, the same authors provided the expressions for both deterministic and indeterministic components [13]. As shown by several researchers the SEA can also be used to predict the transient response of complex systems [14–17]. If the structural system under investigation is with parametric uncertainties, then the SEA method and the hybrid method can be modified with consideration of the parameters describing uncertainties. A thorough discussion on this topic has been provided by Ciciriello and Langley [18, 19]. Yin et al [20] considered fuzzy parameters in the deterministic components. The uncertainty propagation in SEA has been analysed by sensitivity method, vertex method and Legendre orthogonal polynomial based method, more information can be found in Culla et al [21] and Xu et al [22]. Christen et al [23] performed sensitive analysis relating parametric uncertainty in either SEA model coefficients or engineering structural parameters has performed by the Fourier analysis sensitivity test method. For the vibro-acoustic systems with fuzzy and interval parameters, two formulations, which respectively are named as modified perturbation SEA and affine interval perturbation SEA, has been proposed to predict the response and uncertainty propagation by Chen et al [24, 25]. Despite the relevant number of papers - some of which are above-mentioned - devoted to the SEA-based method, it should be noted that all of them have been derived under the assumption of linear behaviour of the subsystems joint components. Several works relating nonlinear systems have been performed in entropy-based SEA models. By introducing the Khinchins entropy, Carcaterra [26] proved that the thermodynamic temperature could be applied to analyse the energy flow in Hamiltonian systems with dead-zone and polynomial nonlinearity under assumption of weak coupling. Then a new description - mixing entropy based on the Khinchins entropy was proposed considering two-degree-of-freedom systems by Sotoudeh [27]. A comprehensive discussion on entropy and analysis for various systems including the nonlinearity has been give by Langley [28]. Contributions to nonlinearity investigation could also be from traditional perspectives of SEA. To explore the energy scattering between frequency bands in nonlinear

build-up system, Spelman and Langley [29] developed a nonlinear SEA formulation. This work separates the modes in each frequency band as subsystem and gives the expressions of the nonlinear CLF as the form of tensor. However, the nonlinear springs considered are set to connect the plates and ground but do not joint the plates, which means that the nonlinear joints effect the energy transfer between subsystems is still to be investigated. The main purpose of the present investigation is to extend the SEA model to systems with nonlinear joint components and to thoroughly consider the relation between the energy transfer, nonlinearity and multi-type joints. To this aim several objectives are proposed: (i) the localised cubic nonlinearity, used to model the junctions, is introduced in both translational and/or torsional springs; and according to the hybrid FE-SEA formulation are considered to be the deterministic components of the dynamic system; (ii) the linearisation process, which is an important part in the nonlinear analysis, under the harmonic loading has been carried out through the method of harmonic balance (MHB); (iii) to validation purpose, a further benchmark model with similar localised nonlinearities and linearisation, by combining both the Lagrange-Rayleigh-Ritz method (LRRM) and the Monte Carlo Simulation (MCS) techniques, is developed. Four different case studies, proposing various built-up plate systems with several set of mixed translational and torsional springs, have been investigates and the most meaningful results discussed.

2. Lagrange-Rayleigh-Ritz-Method and localised nonlinearities

This section focuses on the derivation of the governing equations of the nonlinear built-up plate systems using the LRRM. A cubic localised nonlinearity has been taken into account through the inclusion of both translational and torsional springs into the system. The method of harmonic balance, which for the sake of conciseness is not reported in the following, is used for the linearisation of the governing equations. More information can be found in Ref. [30].

2.1. Nonlinear translational spring

Let's consider the two isotropic, homogeneous and linear elastic rectangular plates coupled by springs, whose geometry and schematic representations are shown in the Fig. 6. In this system, the plates are simply supported and the upper plate is subject to a concentrated harmonic force with a constant direction of vertical downward. Each plate (or subsystem) of the whole dynamic system is randomised by using lumped masses randomly distributed. The LRRM based on the weak-form of governing equations of the bare plate is employed

as solution technique [31, 32]. In this context, the transverse displacement $w(x, y, t)$ can be expansed in a Ritz sense through the following multiplication of eigenfunctions and modal coordinates

$$w(x, y, t) = \sum_{mn} \psi_{mn}(\mathbf{x}) q_{mn}(t) \tag{1}$$

where the modal coordinates q_{mn} are time-dependent functions; ψ_{mn} are mass-normalized shape functions. Generally, these shape functions are selected to satisfy at least the geometric boundary conditions. In terms of the simply-supported plates in the present analysis, the shape functions are given as follows

$$\psi_{mn}(\mathbf{x}) = \frac{1}{\sqrt{M_n}} \sin\left(\frac{m\pi}{a}x\right) \sin\left(\frac{n\pi}{b}y\right) \tag{2}$$

where $M_n = \rho hab/4$ represents the modal mass; a and b are the length of the plates along the x and y axis, respectively. The shape functions satisfy the orthogonality condition. The kinetic energy of the system including the randomly distributed masses on the plates in the Fig. 6 are given as follows

$$\begin{aligned} T = &\frac{1}{2}\sum_{mn} \dot{q}_{1,mn}^2 + \sum_{k=1}^{N_{1,m}} \frac{m_k}{2} \sum_{mn}\sum_{ij} \dot{q}_{1,mn}^2 \dot{q}_{1,ij}^2 \psi_{1,mn}(\mathbf{x}_{m_k}) \psi_{1,ij}(\mathbf{x}_{m_k}) \\ &+ \frac{1}{2}\sum_{mn} \dot{q}_{2,mn}^2 + \sum_{k=1}^{N_{2,m}} \frac{m_k}{2} \sum_{mn}\sum_{ij} \dot{q}_{2,mn}^2 \dot{q}_{2,ij}^2 \psi_{2,mn}(\mathbf{x}_{m_k}) \psi_{2,ij}(\mathbf{x}_{m_k}) \end{aligned} \tag{3}$$

where $N_{1,m}$ and $N_{2,m}$ represent the numbers of random masses on the plates 1 and plate 2, respectively; m_k is the magnitude of the k-th mass; $\mathbf{x}_{m_k} = (x_{m_k}, y_{m_k})$ is the randomised coordinate of the mass m_k. The elastic potential energy of the built-up plate system, is given as follows

$$\begin{aligned} \Phi_e = &\frac{1}{2}\sum_{mn} \omega_{1,mn}^2 q_{1,mn}^2 + \frac{1}{2}\sum_{mn} \omega_{2,mn}^2 q_{2,mn}^2 \\ &+ \sum_{n_s=1}^{Ns} \frac{1}{2} k_{1,n_s} \left[\sum_{mn} \psi_{1,mn}(\mathbf{x}_{k_s}) q_{1,mn} - \sum_{ij} \psi_{2,ij}(\mathbf{x}_{k_s}) q_{2,ij}\right]^2 \\ &+ \sum_{n_s=1}^{Ns} \frac{1}{4} k_{3,n_s} \left[\sum_{mn} \psi_{1,mn}(\mathbf{x}_{k_s}) q_{1,mn} - \sum_{ij} \psi_{2,ij}(\mathbf{x}_{k_s}) q_{2,ij}\right]^4 \end{aligned} \tag{4}$$

where $\omega_{mn} = \sqrt{D/\rho h}((m\pi/a)^2 + (n\pi/b)^2)$ is the natural frequency of the bare plate; D is the flexural rigidity; k_{1,n_s} and k_{3,n_s} correspond to the linear term and the cubic term of n_s-th spring stiffness; $\mathbf{x}_{k_s} = (x_{k_s}, y_{k_s})$ is the coordinates of the joint. The potential energy related

to the application of the external force assumed to be concentrated and perpendicular to the upper plate, as depicted in the Fig. 6, can be written as

$$\Phi_{ext} = \hat{P}_1 \sin(\omega t + \phi) \left[\sum_{mn} \psi_{1,mn}(\mathbf{x}_{P_1}) q_{1,mn} \right] \tag{5}$$

where $\hat{P}_1 \sin(\omega t + \phi)$ represents the sinusoidal excitation with amplitude $\hat{P}_1$, circular frequency ω and phase angle ϕ; $\mathbf{x}_{P_1}$ denotes the coordinate of the external force. The kinetic energy, the elastic potential energy and the potential energy due to the external force can be substituted into the Lagrange's equation

$$\frac{\mathrm{d}}{\mathrm{d}t}\left(\frac{\partial T}{\partial \dot{q}_{mn}}\right) - \frac{\partial T}{\partial q_{mn}} + \frac{\partial \Phi_e}{\partial q_{mn}} = \frac{\partial \Phi_{ext}}{\partial q_{mn}} \tag{6}$$

leading to the following equations of motion,

$$\begin{aligned}
&\ddot{q}_{1,mn} + \omega_{1,mn}^2 q_{1,mn} + \sum_{k=1}^{N_{1,m}} m_k \sum_{ij} \ddot{q}_{1,ij} \psi_{1,ij}(\mathbf{x}_{m_k}) \psi_{1,mn}(\mathbf{x}_{m_k}) \\
&+ \sum_{n_s=1}^{Ns} k_{1,n_s} \left[\sum_{ij} q_{1,ij} \psi_{1,ij}(\mathbf{x}_{n_s}) - \sum_{ij} q_{2,ij} \psi_{2,ij}(\mathbf{x}_{n_s}) \right] \psi_{1,mn}(\mathbf{x}_{n_s}) \\
&+ \sum_{n_s=1}^{Ns} k_{3,n_s} \left[\sum_{ij} q_{1,ij} \psi_{1,ij}(\mathbf{x}_{n_s}) - \sum_{ij} q_{2,ij} \psi_{2,ij}(\mathbf{x}_{n_s}) \right]^3 \psi_{1,mn}(\mathbf{x}_{n_s}) \\
&= \hat{P}_1 \sin(\omega t + \phi) q_{1,mn}
\end{aligned} \tag{7}$$

$$\begin{aligned}
&\ddot{q}_{2,mn} + \omega_{2,mn}^2 q_{2,mn} + \sum_{k=1}^{N_{2,m}} m_k \sum_{ij} \ddot{q}_{2,ij} \psi_{2,ij}(\mathbf{x}_{m_k}) \psi_{2,mn}(\mathbf{x}_{m_k}) \\
&+ \sum_{ns=1}^{Ns} k_{1,n_s} \left[\sum_{ij} q_{2,ij} \psi_{2,ij}(\mathbf{x}_{n_s}) - \sum_{ij} q_{1,ij} \psi_{1,ij}(\mathbf{x}_{n_s}) \right] \psi_{2,mn}(\mathbf{x}_{n_s}) \\
&+ \sum_{ns=1}^{Ns} k_{3,n_s} \left[\sum_{ij} q_{2,ij} \psi_{2,ij}(\mathbf{x}_{n_s}) - \sum_{ij} q_{1,ij} \psi_{1,ij}(\mathbf{x}_{n_s}) \right]^3 \psi_{2,mn}(\mathbf{x}_{n_s}) \\
&= 0
\end{aligned} \tag{8}$$

For convenience the nonlinear response of the system is given in terms of the ensemble-average of the time-averaged vibrational energy, which assumes the following form

$$E[\mathcal{E}_k] = E\left[\frac{1}{T_P} \int_0^{T_P} 2T^{(k)} dt \right] = E\left[2\bar{T}^{(k)} \right] \tag{9}$$

where $E[]$ is the ensemble-average; T_P is the period; $T^{(k)}$ is the kinetic energy of the k-th subsystem; $\bar{T}^{(k)}$ represents the time-averaged kinetic energy.

2.2. Nonlinear Torsional Spring

Similarly, let' s consider the two simply-supported plates coupled by a set of torsional springs depicted in the Fig. 12. Also for this built-up plates system the localised nonlinearity is considered to be cubic. The elastic potential energy of the system can be written as

$$\begin{aligned}\Phi_e = &\frac{1}{2}\sum_{mn}\omega_{1,mn}^2 q_{1,mn}^2 + \frac{1}{2}\sum_{mn}\omega_{2,mn}^2 q_{2,mn}^2 \\ &+ \sum_{n_t=1}^{Nt}\frac{1}{2}k_{n_t}\left[\sum_{mn}\frac{\partial\psi_{1,mn}}{\partial y}\bigg|_{\mathbf{x}=\mathbf{x}_{k_t}} q_{1,mn} - \sum_{ij}\frac{\partial\psi_{2,mn}}{\partial y}\bigg|_{\mathbf{x}=\mathbf{x}_{k_t}} q_{2,ij}\right]^2 \\ &+ \sum_{n_t=1}^{Nt}\frac{1}{4}k_{n_t}\left[\sum_{mn}\frac{\partial\psi_{1,mn}}{\partial y}\bigg|_{\mathbf{x}=\mathbf{x}_{k_t}} q_{1,mn} - \sum_{ij}\frac{\partial\psi_{2,mn}}{\partial y}\bigg|_{\mathbf{x}=\mathbf{x}_{k_t}} q_{2,ij}\right]^4\end{aligned} \tag{10}$$

where $\frac{\partial\psi_{mn}}{\partial y}\Big|_{\mathbf{x}=\mathbf{x}_{k_t}}$ is the partial derivative of the eigenfunction with respect to y coordinate at the junction $\mathbf{x}_{k_t}$. Substituting Eq. (10) and Eq. (3) into Eq. (6) leads to the equations of motions as follows

$$\begin{aligned}&\ddot{q}_{1,mn} + \omega_{1,mn}^2 q_{1,mn} + \sum_{k=1}^{N_{1,m}} m_k \sum_{ij}\ddot{q}_{1,ij}\psi_{1,ij}(\mathbf{x}_{m_k})\psi_{1,mn}(\mathbf{x}_{m_k}) \\ &+ \sum_{n_t=1}^{N_t} k_{1,n_t}\left[\sum_{ij} q_{1,ij}\frac{\partial\psi_{1,ij}}{\partial y}\bigg|_{\mathbf{x}=\mathbf{x}_{n_t}} - \sum_{ij} q_{2,ij}\frac{\partial\psi_{2,ij}}{\partial y}\bigg|_{\mathbf{x}=\mathbf{x}_{n_t}}\right]\frac{\partial\psi_{1,mn}}{\partial y}\bigg|_{\mathbf{x}=\mathbf{x}_{n_t}} \\ &+ \sum_{n_t=1}^{N_t} k_{3,n_t}\left[\sum_{ij} q_{1,ij}\frac{\partial\psi_{1,ij}}{\partial y}\bigg|_{\mathbf{x}=\mathbf{x}_{n_t}} - \sum_{ij} q_{2,ij}\frac{\partial\psi_{2,ij}}{\partial y}\bigg|_{\mathbf{x}=\mathbf{x}_{n_t}}\right]^3\frac{\partial\psi_{1,mn}}{\partial y}\bigg|_{\mathbf{x}=\mathbf{x}_{n_t}} \\ &= \hat{P}_1\sin(\omega t+\phi)q_{1,mn}\end{aligned} \tag{11}$$

$$\begin{aligned}&\ddot{q}_{2,mn} + \omega_{2,mn}^2 q_{2,mn} + \sum_{k=1}^{N_{2,m}} m_k \sum_{ij}\ddot{q}_{2,ij}\psi_{2,ij}(\mathbf{x}_{m_k})\psi_{2,mn}(\mathbf{x}_{m_k}) \\ &+ \sum_{n_t=1}^{N_t} k_{1,n_t}\left[\sum_{ij} q_{2,ij}\frac{\partial\psi_{2,ij}}{\partial y}\bigg|_{\mathbf{x}=\mathbf{x}_{n_t}} - \sum_{ij} q_{1,ij}\frac{\partial\psi_{1,ij}}{\partial y}\bigg|_{\mathbf{x}=\mathbf{x}_{n_t}}\right]\frac{\partial\psi_{2,mn}}{\partial y}\bigg|_{\mathbf{x}=\mathbf{x}_{n_t}} \\ &+ \sum_{n_t=1}^{N_t} k_{3,n_t}\left[\sum_{ij} q_{2,ij}\frac{\partial\psi_{2,ij}}{\partial y}\bigg|_{\mathbf{x}=\mathbf{x}_{n_t}} - \sum_{ij} q_{1,ij}\frac{\partial\psi_{1,ij}}{\partial y}\bigg|_{\mathbf{x}=\mathbf{x}_{n_t}}\right]^3\frac{\partial\psi_{2,mn}}{\partial y}\bigg|_{\mathbf{x}=\mathbf{x}_{n_t}} \\ &= 0\end{aligned} \tag{12}$$

The equations of motions above have similar forms to those with translational nonlinear springs of Eq. (7) and Eq. (8). The main difference occurs in the coupling term with k_{1,n_t} and k_{3,n_t} as a result of the torsional joints. To solve the nonlinear governing equations in Eqs. (7) and (8) and Eqs. (11) and (12), a linearisation procedure is needed.

3. Hybrid FE-SEA formulation accounting for localised nonlinearities

In the present section a concise overview of the hybrid FE-SEA formulation accounting for nonlinearities in the joint components of the dynamic system is provided. The hybrid FE-SEA formulation firstly requires the identification of those components, within the system, which are assumed to behave statistically. These component are modelled as SEA subsystems. The remaining components are deemed to be deterministic and are modelled by using the FE method. The relationship between the SEA and the FE subsystems, is considered to meet the following conditions [8],

$$\mathbf{D}_{tot}\mathbf{q} = \mathbf{f} + \sum_{k} \mathbf{f}_{rev}^{k} \tag{13}$$

$$\mathbf{D}_{tot} = \mathbf{D}_{d} + \sum_{k} \mathbf{D}_{dir}^{k} \tag{14}$$

where $\mathbf{q}$ is the general displacement of FE parts under the frequency of ω; $\mathbf{f}$ represent the external forces exerted to the FE components; $\mathbf{f}_{rev}^{k}$ are the forces resulting from the reverberant field in k-th subsystem; $\mathbf{D}_{d}$ corresponds to the dynamic stiffness matrix of the deterministic components; $\mathbf{D}_{dir}^{k}$ is the the dynamic stiffness matrix arising from k-th direct field. Considering the diffuse field reciprocity relation between direct fields and reverberant fields [33], the energy equilibrium equation for each subsystem and the cross spectral matrix $\mathbf{S}_{qq}$ is given as [7]

$$\omega\left(\eta_{j} + \eta_{d,j}\right) + \sum_{k} \omega\eta_{jk} n_{j} \left(\frac{E_{j}}{n_{j}} - \frac{E_{k}}{n_{k}}\right) = P_{in,j} + P_{in,j}^{ext} \tag{15}$$

$$\mathbf{S}_{qq} = \mathbf{D}_{tot}^{-1}\left[\mathbf{S}_{ff} + \sum_{k}\left(\frac{4E_{k}}{\omega\pi n_{k}}\right)\mathrm{Im}\left\{\mathbf{D}_{dir}^{(k)}\right\}\right]\left(\mathbf{D}_{tot}^{-1}\right)^{*T} \tag{16}$$

where

$$P_{in,j}^{ext} = \left(\frac{\omega}{2}\right)\sum_{rs}\mathrm{Im}\left\{D_{dir,rs}^{j}\right\}\left[\mathbf{D}_{tot}^{-1}\mathbf{S}_{ff}(\mathbf{D}_{tot}^{-1})^{*T}\right]_{rs} \tag{17}$$

$$\eta_{jk} = \frac{2}{\omega\pi n_{j}}\sum_{rs}\mathrm{Im}\left\{D_{dir,rs}^{j}\right\}\left[\mathbf{D}_{tot}^{-1}\mathrm{Im}\left\{\mathbf{D}_{dir}^{(k)}\right\}(\mathbf{D}_{tot}^{-1})^{*T}\right]_{rs} \tag{18}$$

$$\eta_{d,j} = \frac{2}{\omega\pi n_{j}}\sum_{rs}\mathrm{Im}\left\{D_{d,rs}\right\}\left[\mathbf{D}_{tot}^{-1}\mathrm{Im}\left\{\mathbf{D}_{dir}^{(j)}\right\}(\mathbf{D}_{tot}^{-1})^{*T}\right]_{rs} \tag{19}$$

In Eq. (15), η_{j} is the loss factor of j-th subsystem; $\eta_{d,j}$ corresponds to the power dissipation in j-th master system; η_{jk} is the coupling loss factor; n_{j} is the modal density; E_{j} is the ensemble average energy of j-th subsystem; $P_{in,j}$ and $P_{in,j}^{ext}$ represent the power input from the loadings to subsystems and to master systems respectively. In Eq. (16), $\mathbf{S}_{ff}$ denotes

the cross spectral matrix of external forces to master systems. Usually, Eq. (15) and Eq. (16) are used to obtain the response of subsystems and FE components. To solve Eq. (15), $P_{in,j}^{ext}$, η_{jk} and $\eta_{d,j}$ can be calculated by Eqs. (17)-(19). Then the responses of deterministic components are obtained using Eq. (16). As far as the localised nonlinearity is concerned, it is treated exactly in the same manner of the LRRM benchmark model. Namely, the MHB is used for the linearisation of the cubic nonlinearities localised in both translational and/or torsional springs.

4. Numerical results

This section proposes numerical results for four different configurations of built-up plate systems, in order to validate and assess the foregoing developed methodology. Both translational and torsional springs are considered to be joint components of the coupled plates, and can have both linear and nonlinear mechanical behaviour. In all of the addressed case studies a cubic nonlinearity is accounted for. The developed hybrid FE-SEA including localised nonlinearities is employed to obtain the ensemble-average of the time-averaged energy function; and the benchmark model LRRM plus MCS featured by the same set of nonlinear springs is employed for comparison purpose. The system is randomised by using distributed lumped masses. The effectiveness of the randomisation process, through the achievement of universality in the natural frequency distribution of the dynamic system under investigation, has been analysed. In all of the addressed case studies the material is homogeneous, isotropic and linear elastic with Young's modulus $E = 70$GPa; Poisson's ratio $\nu = 0.3$ and density $\rho = 2700\text{kg/m}^3$. The plates' damping loss factor and their size including a and b (plate's sides) as well as h (thickness), are given in the Tab. 1.

4.1. GOE statistics

The GOE statistics is the one underpinning the hybrid FE-SEA formulation, namely, it describes the statistics of the natural frequency spacing in each SEA subsystem. Early works on this subject matter, used to consider the modal spacing as a Poisson process leading to an exponential distribution [34]. This would be correct in systems featured by components/subsystems free of imperfections. In real-life structures, components are made up of materials including voids and defects, and manufacturing imperfections. All of these uncertainties make the mode spacing conform to the GOE statistics based on the Rayleigh distribution. This has been proved both numerically and experimentally [9, 11]. When the

GOE statistics occur, the modes of system might mix and veer in high-frequency range. For purpose of measuring the amount of mixing and veering in the process, a parameter called statistical overlap factor has been defined as follow [9],

$$S = \frac{2\sigma}{\mu} = \frac{2\{var[\Delta\omega_n]\}^{1/2}}{\mu} \tag{20}$$

where σ represents the standard derivation of natural frequency of system with uncertainty; μ denotes the mean spacing of natural frequency; ω_n corresponds to n-th natural frequency. For a simply-supported plate with lumped mass attachments the statistical overlap factor S increases, with a linear trend, while increasing the frequency till reaching a plateau in a well defined frequency range. As this value approaches the unity the GOE statistics occurs. The mean value of the statistical overlap factor $\bar{S}$ identifies a level section which helps in the identification of the correct randomisation scheme to achieve the GOE statistics. The above discussed parameters are thoroughly investigated by analysing the rectangular plate with lumped mass attachments shown in Fig. 1. The geometrical parameters used for the plate are those proposed for plate 1 in Tab. 1. The statistical overlap factor against the circular frequency, and for different number of small masses, is investigated in Fig. 2. It is visible form Fig. 2(a) that for a number of 20 small masses the statistical overlap factor $S > 1$; this is also confirmed by its mean values plotted in Fig. 2(b). This means that a number of 20 lumped mass attachments is enough to randomise the plate to reach the GOE statistics. As the lumped masses weight is also a key parameters to achieve GOE statistics, the mean value of statistical overlap factor is calculated with variation of the masses number and the mass rate in terms of the total weight of the bare plate. The result is shown in Fig. 3. It can be noted that for 20 small masses having the 2% of total weight of the bare plate is $\bar{S} > 1$ assuring that the GOE applies. This is further confirmed by Fig. 4 where the probability distribution of the modal spacing is shown for different values of small masses. It should be noted how the transition form an exponential distribution (1 mass) to a Rayleigh distribution is almost complete with 20 masses. Fig. 5 shows the comparison of the quantiles of a perfect Rayleigh distribution and the one achieved with various value of lumped mass attachments. Once again it can be noted that 20 small masses are sufficient to properly randomise the subsystem. Being the size of plate 2 and plate 3 smaller than those of plate 1 and plate 4, the distribution of the lumped masses on their surface is denser. For all these reasons, the aforementioned values are those that have been selected to simulate the uncertainties within the dynamic system in the benchmark model.

4.2. Built-up plate systems

The first case study is depicted in Fig. 6. The geometrical parameters used for plate 1 and plate 2 are given in Tab. 1. The linear and nonlinear translational spring elastic coefficients are given as: $k_l = 2 \times 10^5$ and $k_{nl} = 2 \times 10^{15}$, respectively. The system is subjected to an harmonic point load of 1000 N acting on plate 1. The results in Fig. 7(a) show the time-averaged energy response of a linear LRRM plus MCS analysis with 200 samples. The MCS analysis for the linearised system leads to a similar trend of the linear one; so for the sake of conciseness only the ensemble-average has been shown. Fig. 7(b) compares the ensemble-average of the time-averaged energy response of both linear and linearised systems, computed by using both the LRRM plus MCS and the hybrid FE-SEA formulation. In all of the mentioned analysis the results show an excellent agreement. As expected the introduction of the nonlinearity increases the energy level in the ensemble-average energy response of plate 2 due to the stiffening effect induced in the translational springs. In order to validate if the probability distribution of ensemble energy response of the subsystems is log-normal in terms of nonlinear LRRM plus MCS formulation, Fig. 8 compares the distribution of linear and linearised analysis at the circular frequency $\omega = 4000$ (rad/s). It can be observed that logarithm of the energy responses of the subsystems yielded by both linear and linearised analysis are consistent with normal distribution, which means the MCS samples conform to the a log-normal distribution showing and excellent match for the linear analysis and a good one for the linearised analysis. A similar result can be noted in Fig. 9 where the quantiles of a log-normal distribution are compared with those of the MSC samples. Moreover, from the MCS the 99% confidence interval of the ensemble-average energy response is computed. In regards of that, Fig. 10 shows the ensemble-average energy response predicted by linear and linearised hybrid FE-SEA formulation is within the interval estimated by the benchmark in most circular frequency range. In Fig. 11 the effect of the of both linear and nonlinear spring stiffness coefficients is examined. More specifically, in Fig. 11(a) as expected the ensemble-average energy response increases uniformly while increasing, by an order of magnitude at each analysis ($k_l = 2 \times 10^2, 2 \times 10^3, 2 \times 10^4, 2 \times 10^5$), the linear spring stiffness coefficient and keeping constant the nonlinear one $k_{nl} = 2 \times 10^{15}$. In Fig. 11(b) the same analysis is performed but rising the nonlinear spring stiffness coefficient ($k_{nl} = 2 \times 10^9, 2 \times 10^{11}, 2 \times 10^{13}, 2 \times 10^{15}$) with the linear one constant $k_l = 2 \times 10^4$. The increase of the nonlinear stiffness coefficients leads to different increment in high-frequency range and lower-frequency range. Smaller nonlinear

coefficient affect significantly the ensemble-average energy response at lower-frequencies but have little effects on higher-frequencies. This is related to the fact that the displacement in lower-frequency range is larger than that in higher-frequency range and the cubic nonlinearity amplifies it. Moreover, the difference in the ensemble-average energy response with the two values $k_{nl} = 2 \times 10^{13}$ and $k_{nl} = 2 \times 10^{15}$ is slightly noted at higher-frequencies but coincides at the lower ones. This is due to the fact that the translational springs with those high values of the nonlinear stiffness coefficients behave like rigid joint components.

The second case study is shown in Fig. 12 it consists of a buid-up plate system made up of plate 1 and plate 2, as shown in Tab. 1, and torsional springs whose linear and nonlinear stiffness coefficients are given as $k_{\theta l} = 10^3$ and $k_{\theta nl} = 10^{12}$, respectively. The dynamic system is loaded exactly in the same way of the case study 1. As for the previous case the entire ensemble is shown in Fig. 13(a) and just for the linear analysis. Once again, as shown in Fig. 13(b), the hybrid FE-SEA formulation turned out to be extremely accurate in the prediction the correct ensemble-average energy response, for both the linear and the linearised analysis. It should also be noted that the torsional springs' connection is more stable and smooth than the one made up of translational springs; this can be observed in the slightly oscillatory ensemble response and ensemble-average energy response computer via LRRM plus MCS.

The third case study is schematically shown in Fig. 14. The geometrical parameters of plate 1, 2 and 3 could be found in Tab. 1 and the linear and nonlinear stiffness coefficient of translational springs and torsional springs are provided in the case studies 1 and 2 before the parametric analysis. Four different scenarios are considered: i) Both translational and torsional springs are linear; ii) nonlinearity introduced only in the torsional springs; iii) nonlinearity introduced only in the translational springs; and iv) nonlinearity introduced in both sets of springs. It is clear that the ensemble-average energy response yielded by both linear and linearised hybrid FE-SEA formulation is well-predicted by comparison with that evaluated by the benchmark model. The interaction of the two different sets of springs does not affect the results accuracy.

The fourth case study is related to a four-plate built-up system coupled by two sets of translational springs and two sets of torsional springs (see Fig. 16). The dynamic system is featured by a closed-loop, which might result in change of energy flow path because of the existence of nonlinearity. Similarly to the third case study, four different situations are taken into account and they have been shown in Fig. 17. Compared with the linear analysis shown

in Fig. 17(a), the ensemble-average energy responses given by the linearised hybrid FE-SEA and LRRM plus MCS formulation are illustrated in Fig. 17(b)(c)(d), respectively, considering nonlinearity existing in spring sets 1, spring set 4 and both set 1 and 4, respectively. As can be seen in Fig. 17(b)(c), the nonlinearity narrows the gap of energy response between plate 3 and plate 4, while in Fig. 17(d), at lower frequency, the energy in plate 3 is smaller than that in plate 4 (energy flow path: plate 1→2→3 and 1→4→3), but the reverse happens in high-frequency range (energy flow path: plate 1→2→3→4 and 1→4). Also, expectedly, Fig. 17 shows good agreement between both linear and linearised hybrid FE-SEA and LRRM plus MCS formulations.

5. Conclusion

A hybrid FE-SEA method accounting for nonlinearities in the deterministic components of the system has been developed. The linearisation of the nonlinear deterministic components of the investigated built-up plate systems has been carried out by means of the MHB. The results in terms of ensemble-average of the time-averaged vibrational energy have been compared with those obtained by a linearised LRRM plus MCS method, where the MHB has also been used for the linearisation. Validation and assessment of the proposed formulation has been carried out through four dynamic systems increasingly more complex. In order to find a proper trade-off between computational cost and accuracy within the benchmark formulation, a thorough analysis based on the statistical overlap factor to estimate the right degree of randomness to add at the dynamic system to achieve GOE statistics has been performed. In addition, the convergence analysis carried out to evaluate the appropriate dimension of the computational ensemble led to 50 samples. All of the addressed investigations suggested that the developed hybrid FE-SEA formulation accounting for nonlinear joints leads to a high level of accuracy when compared to the benchmark model, while reducing significantly the computational cost. Since the benchmark model involves solving the integral equations, with a large number of degrees of freedoms, along with the MCS while the SEA model is described by algebraic equations as Eq. (15) with just several orders, it follows that the hybrid FE-SEA formulation can save a significant amount of computational time. To this aim, a comparison of the the computational time for the nonlinear analysis from case 1 to case 4 can be found in the Tab. 2. Moreover, as expected the nonlinearity produced a stiffening effect on the employed sets of springs leading to a higher level of the ensemble-average energy

response in all of the subsystem not driven by the harmonic point load. The MHB turned out to be an effective as well as efficient technique for the system linearisation. Also, both linear and nonlinear sets of torsional springs provide a more stable and smooth connection amongst subsystems; this can be noted by the less oscillatory ensemble and ensemble-average energy response with respect to the ones obtained by using the translational springs.

6. Acknowledgements

The first author wishes to deeply thank Prof. R. S. Langley for the many fruitful and inspiring discussions on the hybrid finite element-statical energy analysis formulation.

Tables

Table. 1. Plate geometrical parameters.

Plate	Edge a (m)	Edge b (m)	Thickness (mm)	Loss factor η	Modal density (modes/Hz)
1	1.35	1.2	5	0.01	0.0942
2	1.05	1.2	15	0.01	0.0245
3	1.05	1.2	5	0.01	0.0733
4	1.35	1.2	5	0.03	0.0942

Table. 2. Computational time for linearised analysis. Computer specifications: Windows 10; processor: Intel(R) Core(TM) i5-8300H CPU @ 2.30GHz; memory: 8.00 GB; system type: 64-bit operating system, x64-based processor; software: MATLAB R2019b.

Case study	Benchmark with 50 MCS samples (s)	Linearised hybrid model (s)
1	172.27	1.02
2	254.32	0.56
3	865.93	1.50
4	1914.45	15.16

Figures

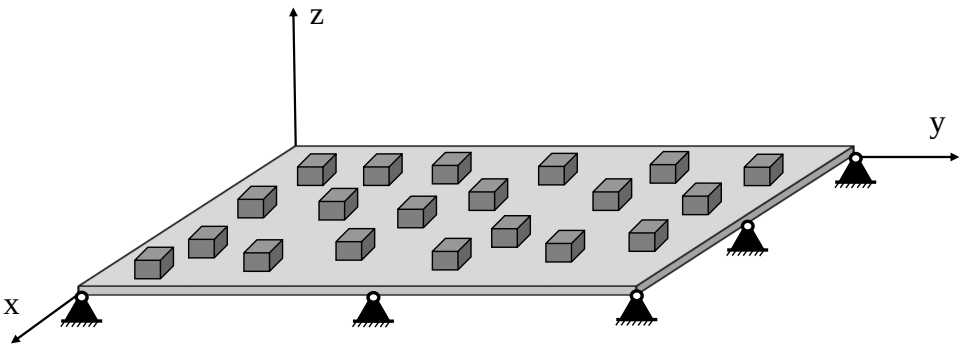

Figure 1. Simply-supported plate with lumped mass attachments.

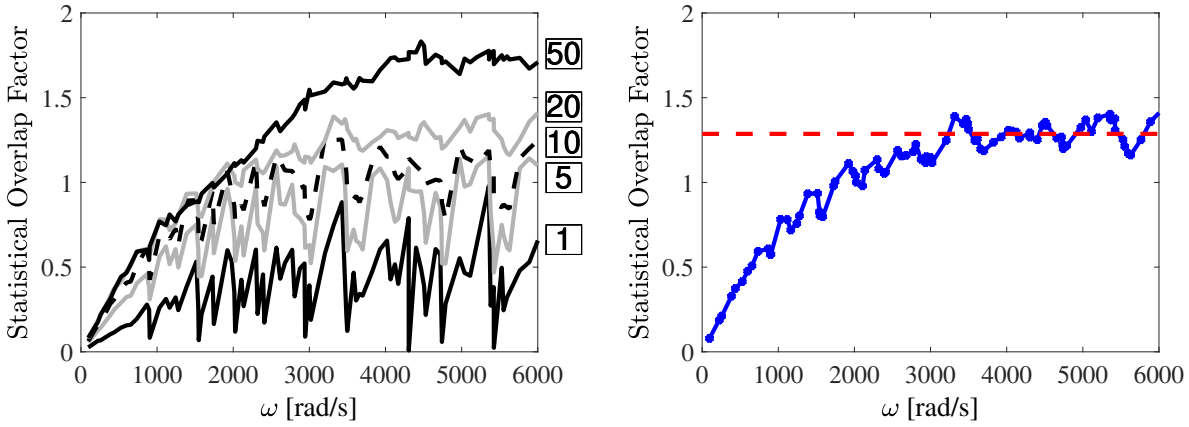

Figure 2. (a) Statistical overlap factor considering 1, 5, 10, 20 and 50 masses; (b) Statistical overlap factor (blue curve) and its mean value of level section (red dashed line) for plate with 20 small masses

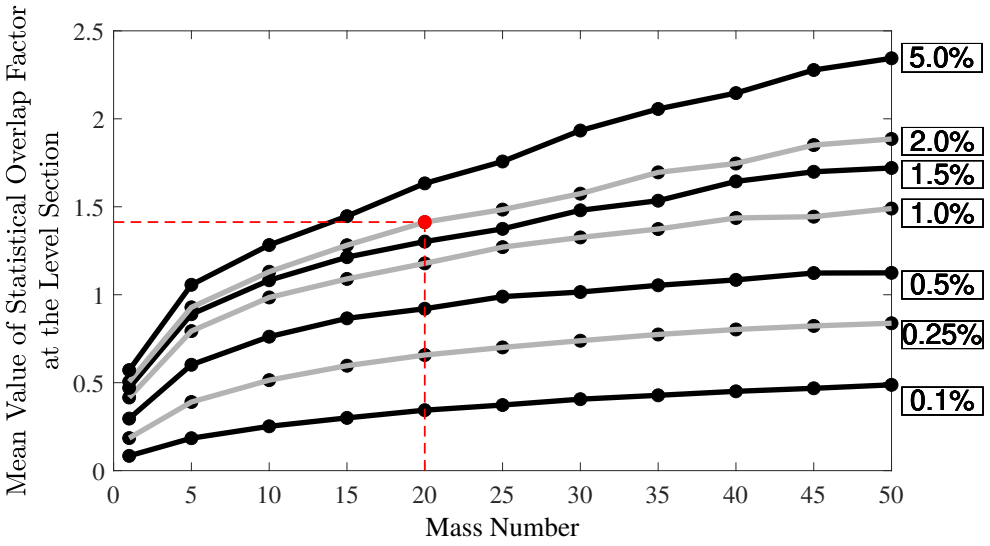

Figure 3. Mean value of the statistical overlap factor with different small mass numbers and percentage weight of the bare plate.

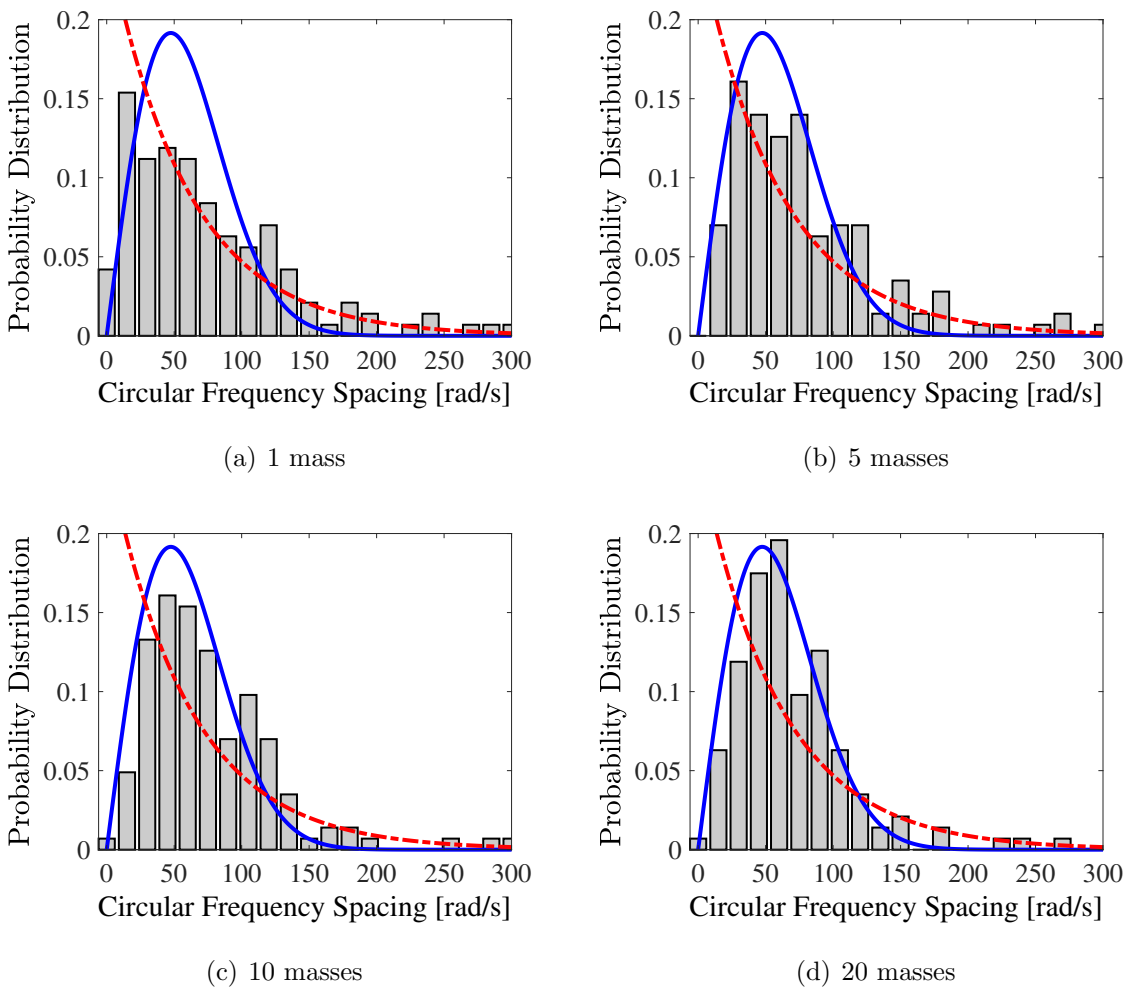

(a) 1 mass

(b) 5 masses

(c) 10 masses

(d) 20 masses

Figure 4. Modal spacing probability distribution. Red curve: exponential distribution; Blue curve: Rayleigh distribution; Grey bar: simulation results.

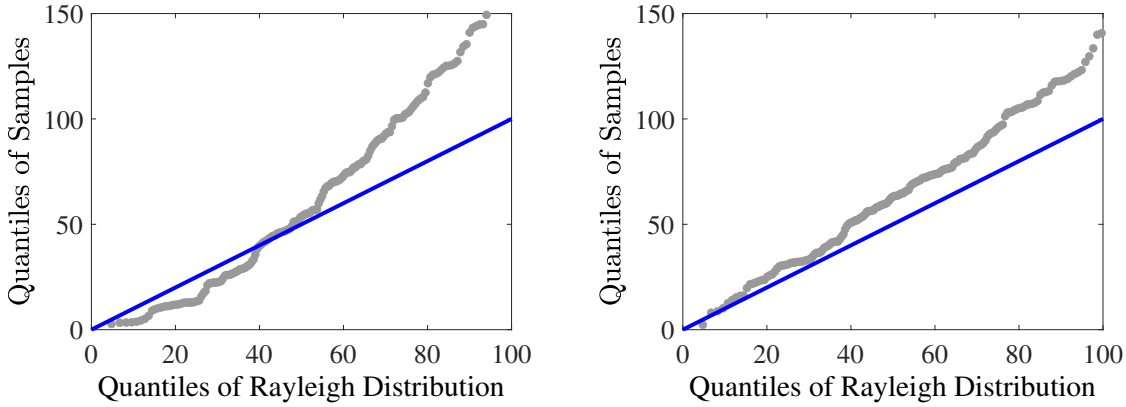

(a) 1 mass

(b) 5 masses

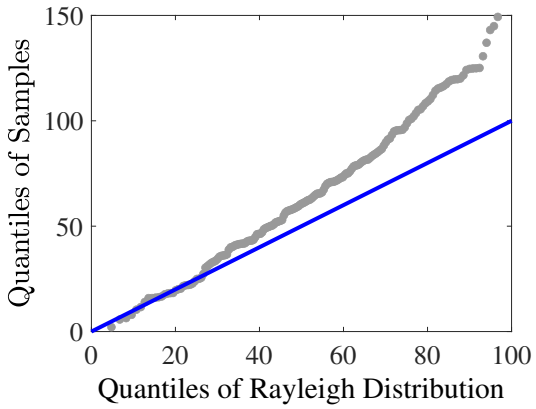

(c) 10 masses

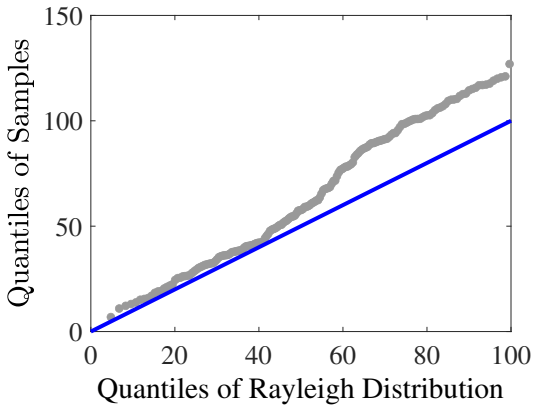

(d) 20 masses

Figure 5. Quantiles of Rayleigh distribution (blue line) versus quantiles from the samples (grey dot) with lumped mass number of 1, 5, 10 and 20.

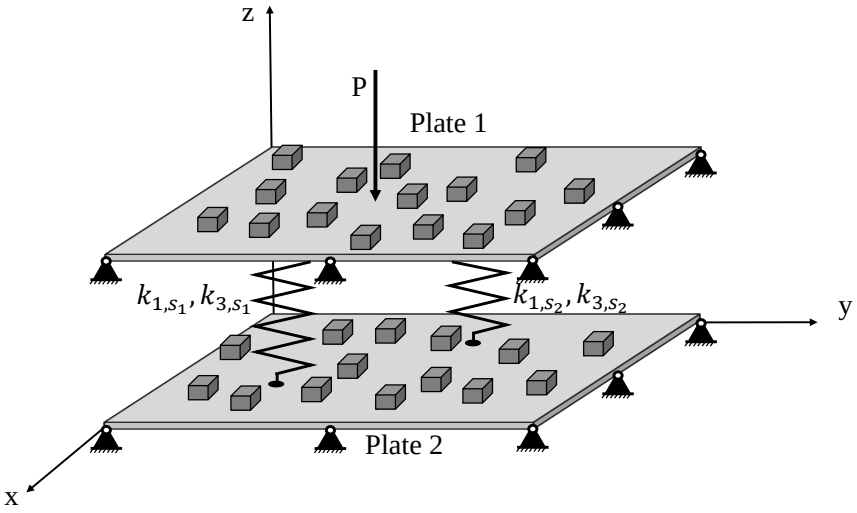

Figure 6. Case study 1: built-up plate system with lumped mass attachments and nonlinear translational springs.

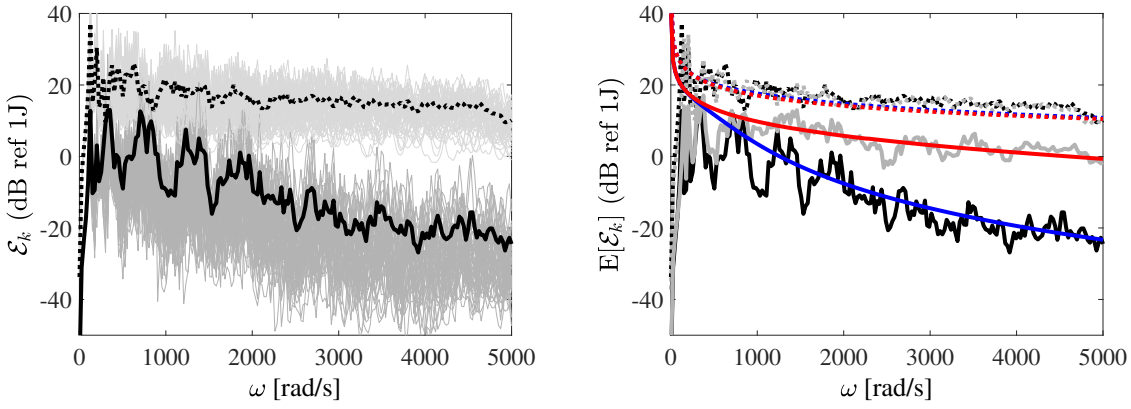

(a) LRRM+MCS linear analysis

(b) Linear and linearised analysis

Figure 7. Vibrational energy response. (a) Light and bold grey cloud: MCS samples of plate 1 and plate 2, respectively; dotted black curve: response of plate 1; solid black curve: response of plate 2. (b) Dotted lines: the response of plate 1; solid lines: of plate 2; the black: linear LRRM+MCS analysis; the grey: linearised LRRM+MCS analysis; the blue: linear FE-SEA analysis; the red: linearised FE-SEA analysis.

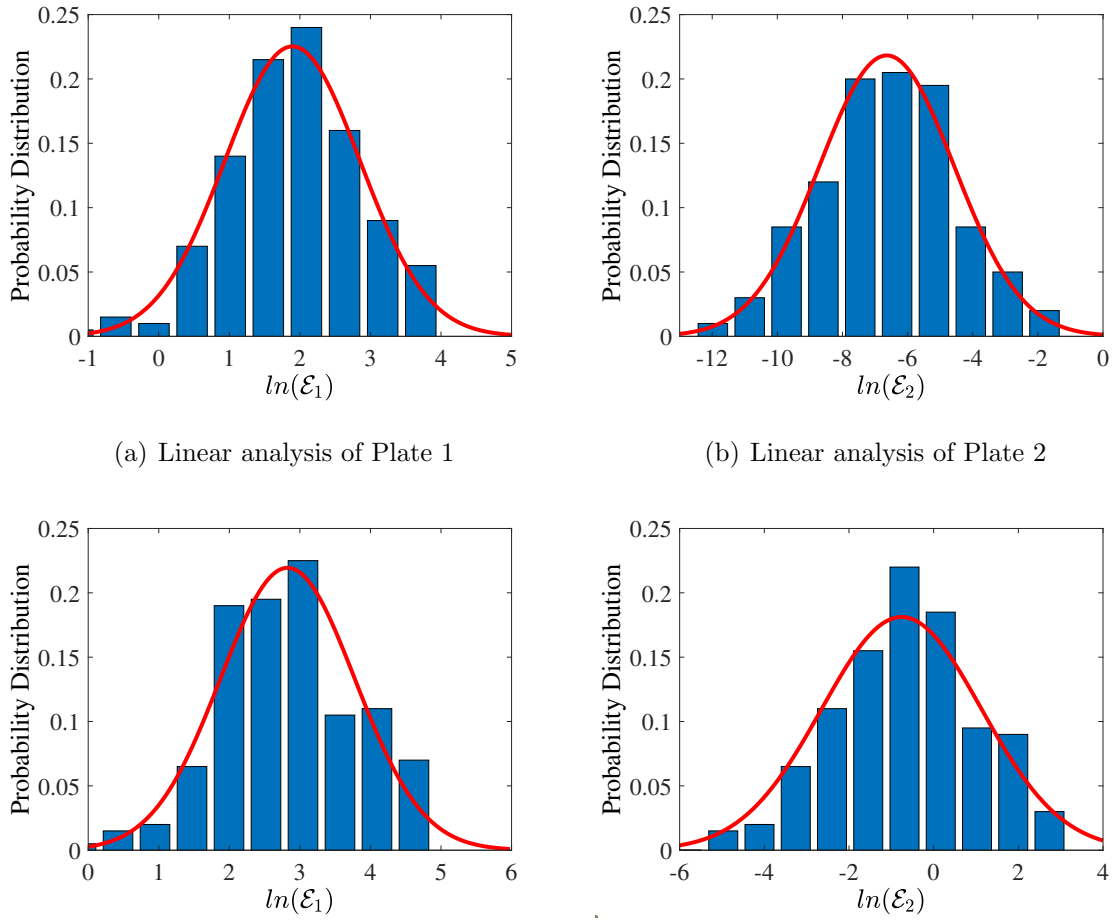

(a) Linear analysis of Plate 1

(b) Linear analysis of Plate 2

(c) Linearised analysis of Plate 1

(d) Linearised analysis of Plate 2

Figure 8. Probability distribution of ensemble vibrational energy response at the frequency of 4000 rad/s. Blue bar: LRRM+MCS simulation; Red curve: normal distribution.

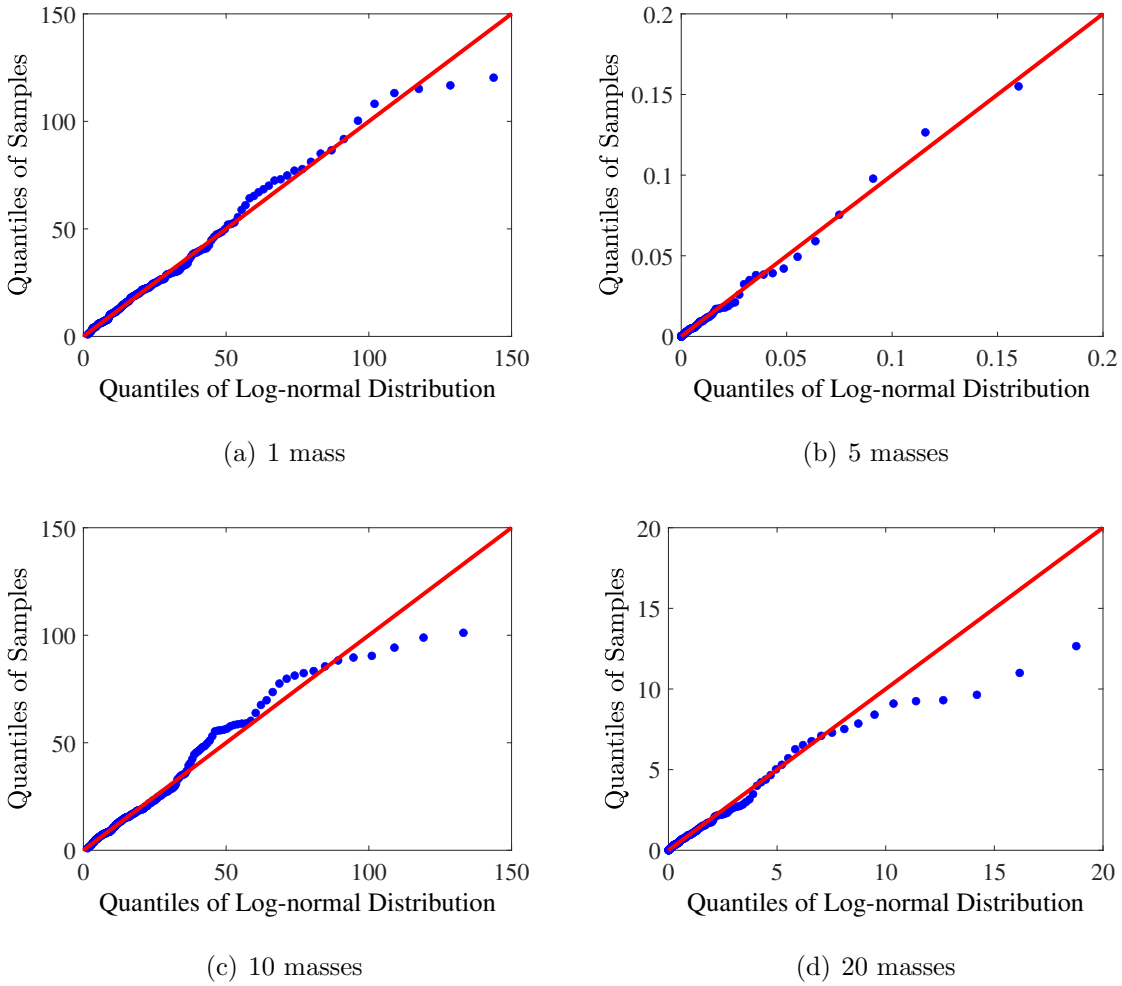

(a) 1 mass

(b) 5 masses

(c) 10 masses

(d) 20 masses

Figure 9. Quantiles of log-normal distribution (red line) versus quantiles from the MCS samples (Blue dot) at 4000 rad/s.

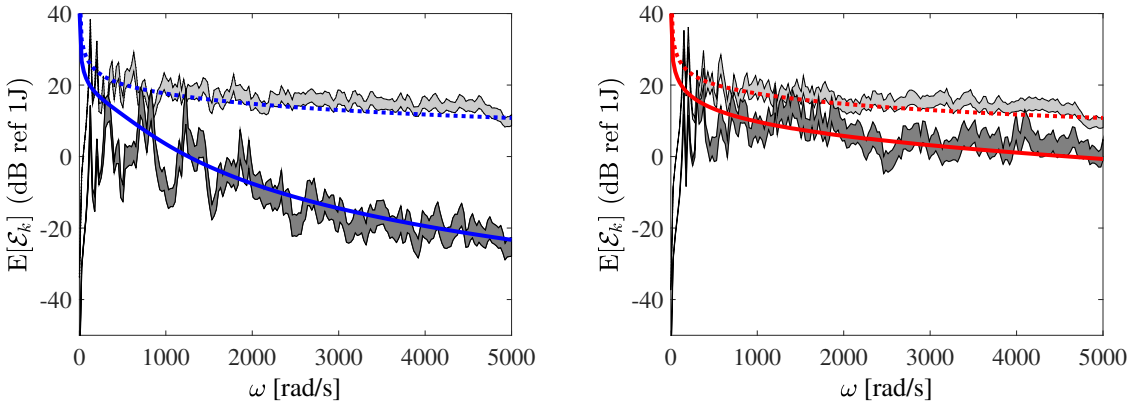

(a) 99% confidence interval for linear analysis (b) 99% confidence interval for linearised analysis

Figure 10. (a) blue curve: FE-SEA analysis; the dotted black: 99% confidence interval for the plate 1; the solid black: for the plate 2; (b) red curve: linearised FE-SEA analysis; the dotted grey: 99% confidence interval for the plate 1; the solid grey: for the plate 2.

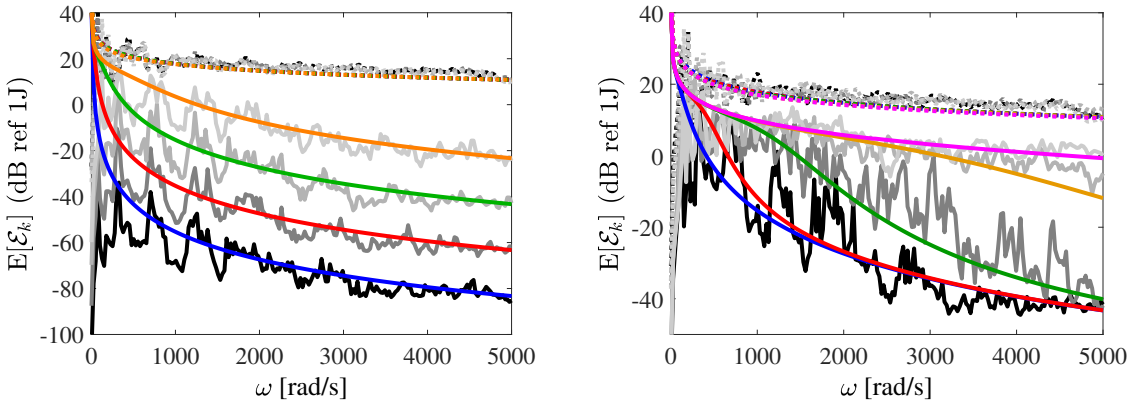

(a) Increasing linear stiffness coefficient (b) Increasing nonlinear stiffness coefficient

Figure 11. (a) Dotted and solid line: for the ensemble-average vibrational energy response of plate 1 and plate 2; blue, red, green and orange curves: linearised FE-SEA responses of spring with increasing linear stiffness coefficient (2×10^2, 2×10^3, 2×10^4 and 2×10^5); from bold curve to the lightest grey: linearised LRRM+MCS analysis. (b) the blue: linear FE-SEA analysis; the red, green, orange and pink: linearised FE-SEA analysis with increasing nonlinear stiffness coefficient (2×10^9, 2×10^{11}, 2×10^{13} and 2×10^{15}); from black curve to the lightest grey: linearised LRRM+MCS analysis.

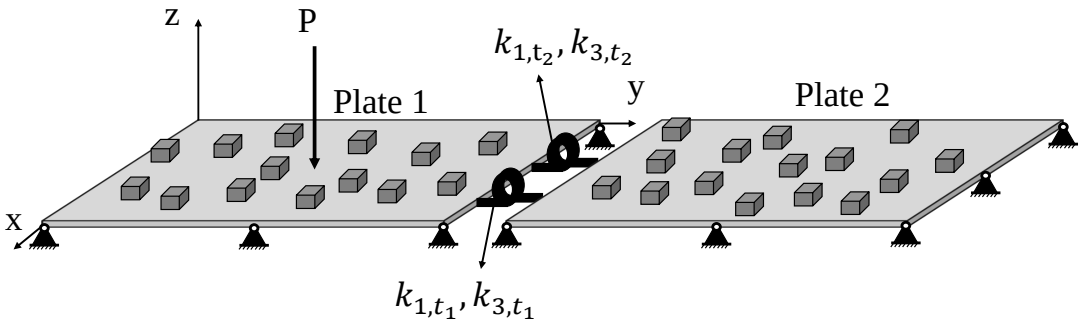

Figure 12. Case study 2: built-up plate system with random masses and nonlinear torsional springs

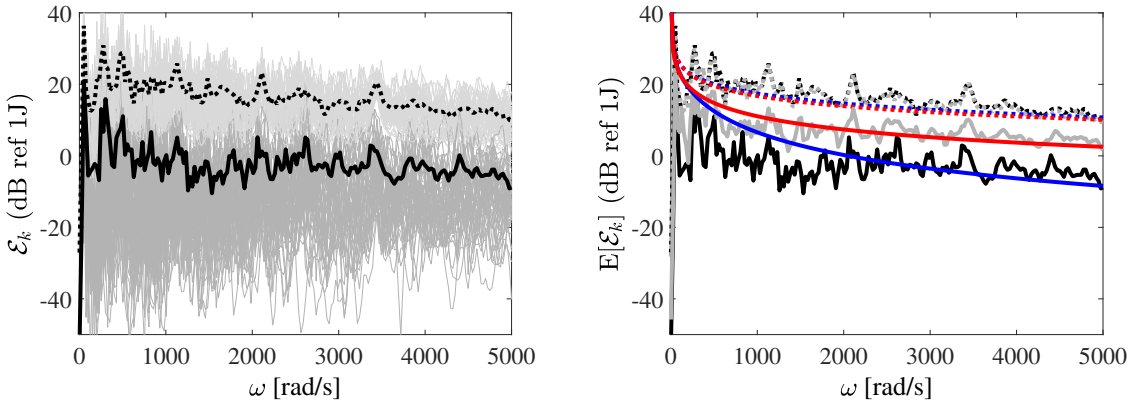

(a) LRRM+MCS linear analysis

(b) Linear and linearised analysis

Figure 13. Vibrational energy response. (a) Light and bold grey cloud: MCS samples of plate 1 and plate 2; dotted black curve: average energy of plate 1; solid black curve: of plate 2. (b) Dotted lines: the response of plate 1; solid lines: of plate 2; the black: linear LRRM+MCS analysis; the grey: linearised LRRM+MCS analysis; the blue: linear FE-SEA analysis; the red: linearised FE-SEA analysis.

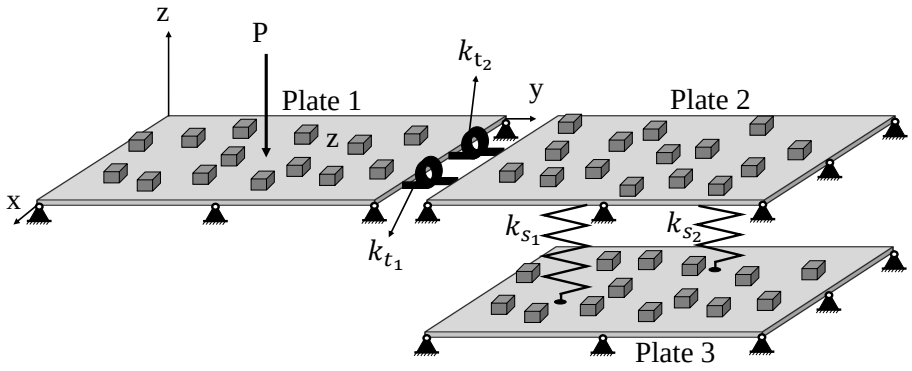

Figure 14. Case study 3: three-plate system with both translational and torsional springs

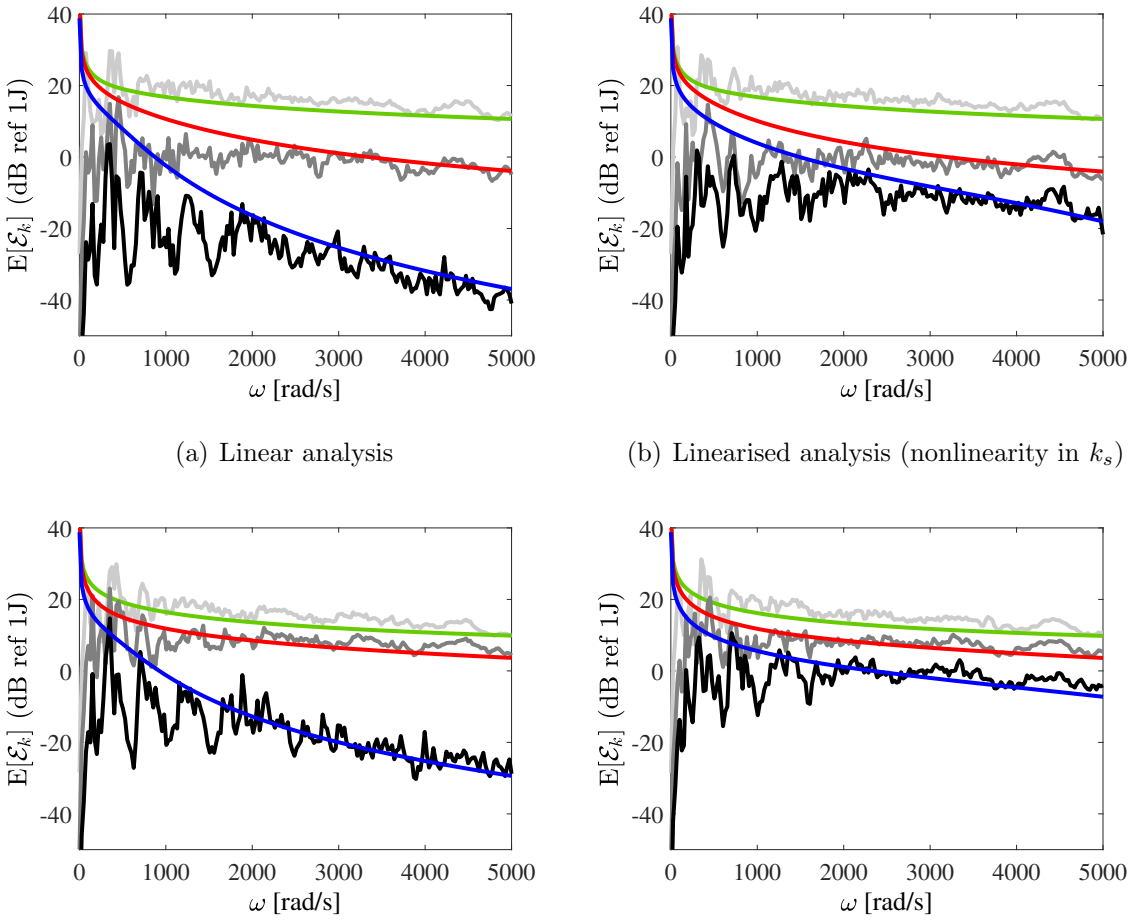

(a) Linear analysis

(b) Linearised analysis (nonlinearity in k_s)

(c) Linearised analysis (nonlinearity in k_t)

(d) Linearised analysis (nonlinearity in k_t and k_s)

Figure 15. Ensemble-average vibrational energy response of linearised FE-SEA and LRRM+MCS analysis of plate 1 (green and light grey), plate 2 (red and dark grey) and plate 3 (blue and black).

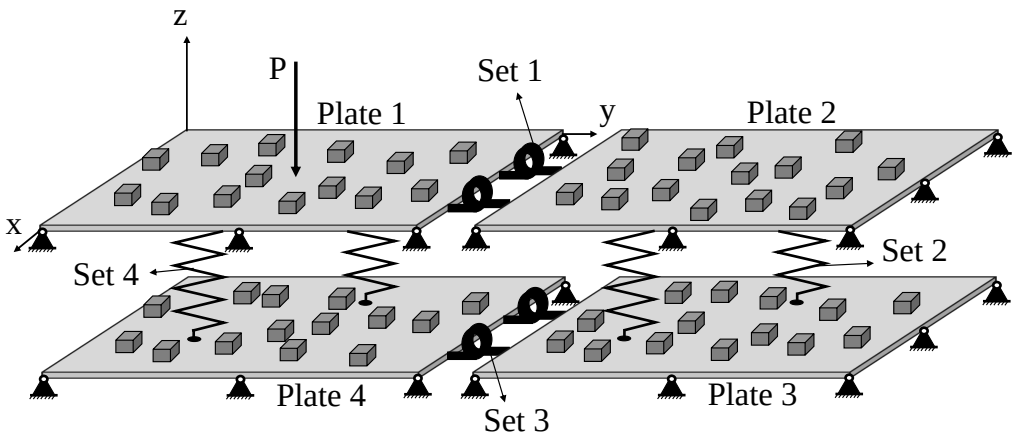

Figure 16. Case study 4: built-up plate system including two translational spring sets and two torsional spring sets.

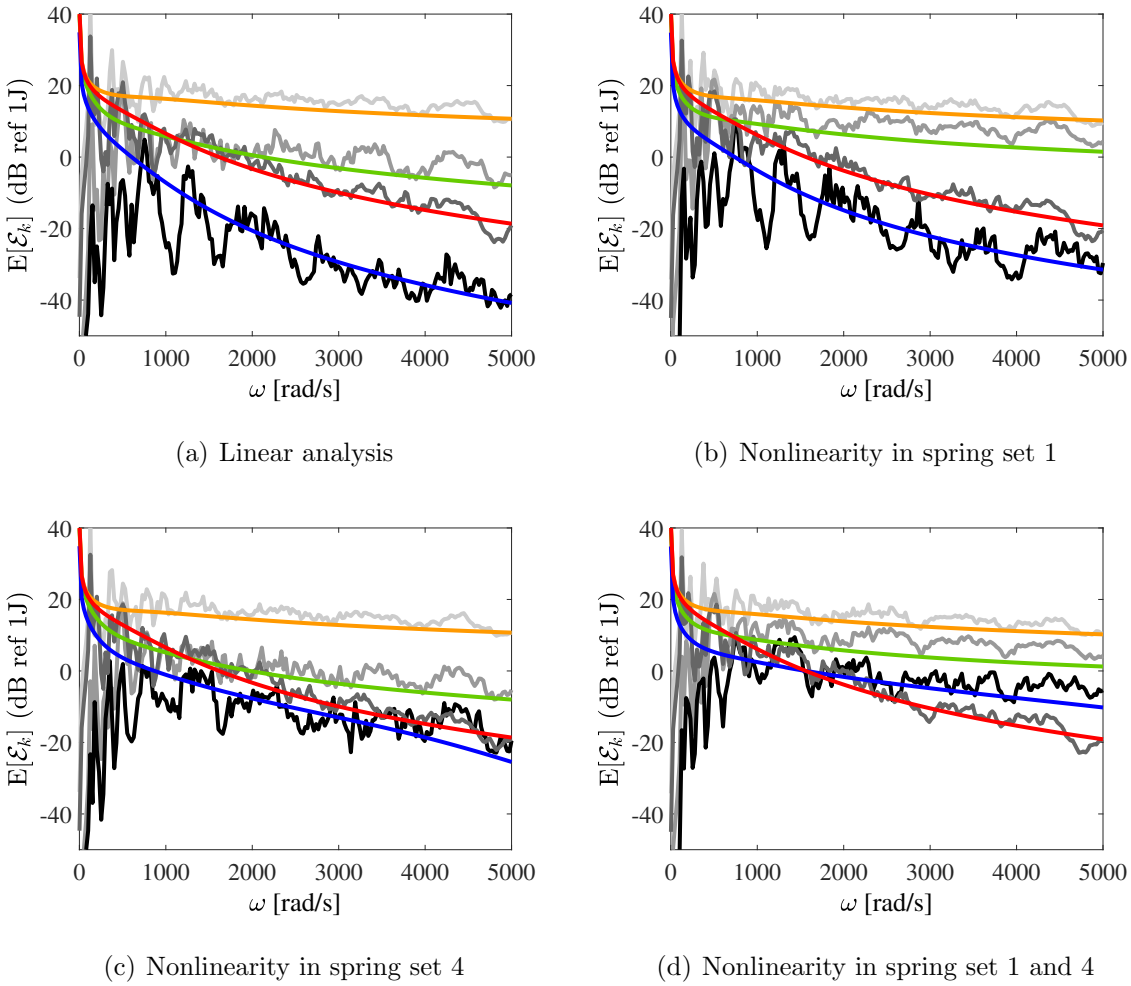

(a) Linear analysis

(b) Nonlinearity in spring set 1

(c) Nonlinearity in spring set 4

(d) Nonlinearity in spring set 1 and 4

Figure 17. Ensemble-average vibrational energy response. The orange, green, red and blue lines: linearised FE-SEA analysis of plate 1, plate 2, plate 4 and plate 3; curves from the lightest grey to the black: linearised LRRM+MCS analysis of the plates.

References

[1] R. H. Lyon. Statistical energy analysis of dynamical systems. *Theory and Applications*, 1975.

[2] J. Fahy. *Statistical Energy Analysis: An overview with applications in structural dynamics*, chapter Chapter 1. Cambridge University Press University press, Cambridge, 1994.

[3] C. H. Hodges and J. Woodhouse. Theories of noise and vibration transmission in complex structures. *Reports on Progress in Physics*, 49(2):107, 1986.

[4] R. S. Langley. A general derivation of the statistical energy analysis equations for coupled dynamic systems. *Journal of Sound and Vibration*, 135(3):499–508, 1989.

[5] R. S. Langley. A derivation of the coupling loss factors used in statistical energy analysis. *Journal of Sound and Vibration*, 141(2):207–219, 1990.

[6] R. S. Langley and P. Bremner. A hybrid method for the vibration analysis of complex structural-acoustic systems. *The Journal of the Acoustical Society of America*, 105(3):1657–1671, 1999.

[7] P. J. Shorter and R. S. Langley. Vibro-acoustic analysis of complex systems. *Journal of Sound and Vibration*, 288(3):669–699, 2005.

[8] V. Cotoni, P. J. Shorter, and R. S. Langley. Numerical and experimental validation of a hybrid finite element-statistical energy analysis method. *The Journal of the Acoustical Society of America*, 122(1):259–270, July 2007.

[9] N. J. Kessissoglou and G. I. Lucas. Gaussian orthogonal ensemble spacing statistics and the statistical overlap factor applied to dynamic systems. *Journal of Sound and Vibration*, 324(3-5):1039–1066, 2009.

[10] R. H. Lyon, R. G DeJong, and M. Heckl. Theory and application of statistical energy analysis, 1995.

[11] R. S. Langley and V. Cotoni. Response variance prediction in the statistical energy analysis of built-up systems. *The Journal of the Acoustical Society of America*, 115(2):706–718, 2004.

[12] V. Cotoni, R. S. Langley, and M. R. F. Kidner. Numerical and experimental validation of variance prediction in the statistical energy analysis of built-up systems. *Journal of Sound and Vibration*, 288(3):701–728, 2005.

[13] R. S. Langley and V. Cotoni. Response variance prediction for uncertain vibro-acoustic systems using a hybrid deterministic-statistical method. *The Journal of the Acoustical Society of America*, 122(6):3445–3463, 2007.

[14] M. L. Lai and A. Soom. Statistical energy analysis for the time-integrated transient response of vibrating systems. 1990.

[15] R. S. Langley, D. Hawes, T. Butlin, and Y. Ishii. Transient sea: Mean and variance predictions. In *INTER-NOISE and NOISE-CON Congress and Conference Proceedings*, volume 257, pages 354–365. Institute of Noise Control Engineering, 2018.

[16] R. S. Langley, D. H. Hawes, T. Butlin, and Y. Ishii. A derivation of the transient statistical energy analysis (tsea) equations with benchmark applications to plate systems. *Journal of Sound and Vibration*, 445:88–102, 2019.

[17] R. S. Langley, D. H. Hawes, T. Butlin, and Y. Ishii. Response variance prediction using transient statistical energy analysis. *The Journal of the Acoustical Society of America*, 145(2):1088–1099, 2019.

[18] A. Cicirello and R. S. Langley. The vibro-acoustic analysis of built-up systems using a hybrid method with parametric and non-parametric uncertainties. *Journal of Sound and Vibration*, 332(9):2165–2178, 2013.

[19] A. Cicirello and R. S. Langley. Efficient parametric uncertainty analysis within the hybrid finite element/statistical energy analysis method. *Journal of Sound and Vibration*, 333(6):1698–1717, 2014.

[20] H. Yin, D. Yu, S. Yin, and B. Xia. Fuzzy interval finite element/statistical energy analysis for mid-frequency analysis of built-up systems with mixed fuzzy and interval parameters. *Journal of Sound and Vibration*, 380:192–212, 2016.

[21] A. Culla, W. DAmbrogio, and A. Fregolent. Parametric approaches for uncertainty propagation in sea. *Mechanical Systems and Signal Processing*, 25(1):193–204, 2011.

[22] M. Xu, Z. Qiu, and X. Wang. Uncertainty propagation in sea for structural–acoustic coupled systems with non-deterministic parameters. *Journal of Sound and Vibration*, 333(17):3949–3965, 2014.

[23] J. L. Christen, M. Ichchou, B. Troclet, O. Bareille, and M. Ouisse. Global sensitivity analysis and uncertainties in sea models of vibroacoustic systems. *Mechanical Systems and Signal Processing*, 90:365–377, 2017.

[24] Q. Chen, Q. Fei, S. Wu, and Y. Li. Uncertainty propagation of the energy flow in vibro-acoustic system with fuzzy parameters. *Aerospace Science and Technology*, 94:105367, 2019.

[25] Q. Chen, Q. Fei, S. Wu, and Y. Li. Statistical energy analysis for the vibro-acoustic system with interval parameters. *Journal of Aircraft*, 56(5):1869–1879, 2019.

[26] A. Carcaterra. Thermodynamic temperature in linear and nonlinear hamiltonian systems. *International Journal of Engineering Science*, 80:189–208, 2014.

[27] Z. Sotoudeh. Entropy and mixing entropy for weakly nonlinear mechanical vibrating systems. *Entropy*, 21(5):536, 2019.

[28] R. S. Langley. On the statistical mechanics of structural vibration. *Journal of Sound and Vibration*, 466:115034, 2020.

[29] G. M. Spelman and R. S. Langley. Statistical energy analysis of nonlinear vibrating systems. *Philosophical Transactions of the Royal Society A: Mathematical, Physical and Engineering Sciences*, 373(2051):20140403, 2015.

[30] K. Worden and G. R. Tomlinson. *Nonlinearity in Structural dynamics*. IoP, Institute of Physics Publishing Bristol and Philadelphia, 2001.

[31] F. A. Fazzolari and R. S. Langley. The statistical energy analysis of systems with nonlinear joints. In *24th International Congress on Sounds and Vibration*, London, 24-27, July, 2017.

[32] F. A. Fazzolari. A hybrid finite element-statistical energy analysis formulation accounting for nonlinearities. In *13th International Conference on Computing Sstructures Technologies*, barcelona, 4-6, September, 2018.

[33] P. J. Shorter and R. S. Langley. On the reciprocity relationship between direct field radiation and diffuse reverberant loading. *The Journal of the Acoustical Society of America*, 117 1:85–95, 2005.

[34] R. H. Lyon. Statistical analysis of power injection and response in structures and rooms. *The Journal of the Acoustical Society of America*, 45(3):545–565, 1969.

*Detailed Response to Reviewers

Reply letter to reviewer 1

The authors thank the reviewer for accepting the paper. It is also grateful that the reviewer's suggestions mentioned in the first round help much to improve the quality of this paper.

Reply letter to reviewer 2

The authors deeply thanks this reviewer for providing constructive suggestions. A point-to-point reply can be found in the follows.

- There exist many potential applications in structural dynamics for the formulation proposed in this paper, but this paper focuses on the theoretical investigation and the validation. This paper has derived the formulation and validated it by applying built-up systems with nonlinear joints, as is mentioned in the title. One further work is to extend this formulation to real-life structures like ship structure or vehicle structure.

- The authors have checked the paper again according to the previous reviewer's comments. Some errors have been found and corrected. Please see the revision lists.

- The universality of Gaussian Orthogonal Ensemble (GOE) statistics has been shown in the subsection 4.1. The figures (Fig. 2, 4 and 5) have illustrated how the statistical overlap factor vary and how the modes are distributed when there exists uncertainties. All these results conform to basic assumptions in the engineering, for instance, the modes of uncertain plate follow the Rayleigh distribution.

  To prove the universality of the formulation proposed, the authors have chosen typical case studies and in this paper applied as many as four case studies from the simple to the increasingly complex including translational or/and torsional springs. The authors believe these four case studies along with the corresponding discussion are enough to illustrate the universality.

***Style Checklist**

Journal of Sound and Vibration

Author Checklist

Authors should complete the following checklist and submit with their revised manuscript.

Math notation follows requirements on Guide for Authors (GFA) see: ☒

https://www.elsevier.com/journals/journal-of-sound-and-vibration/0022-460X/guide-for-authors

Use Roman (normal upright) type for: Total differential operators (e.g. d in differential); i or j (square root of -1); exp or e (base of natural logarithms); Re or Im (real or imaginary part); log, ln, sin, cos, etc.; abbreviations such as c.c. (complex conjugate); multiletter symbols (e.g. TL for transmission loss); subscripts of two or more letters identifiable as words or word-abbreviations (e.g., Apipe, fmax) ☒

For more unusual functions, JSV follows Abramowitz and Stegun's book. More detail given in the GFA (see link above).

Unit symbols - These should be upright (e.g. kg, not *kg*). ☒

All authors are listed on the manuscript with correct affiliations, correct email address and are in correct order. ☒

Keywords present. ☒

Manuscript is not currently submitted to any other Journal. ☒

If submitting highlights please note that only six may be submitted and each one should be no longer than 85 characters in length. ☒

Novelty of paper has been clearly stated in the Introduction. ☒

References are presented as per GFA. ☒

References not produced in English language to have English translation in brackets. ☒

Figures and Tables and Equations are numbered in sequence correctly. (See GFA). ☒

Nomenclature (if required) appears on second page of submission. ☒

Acknowledgements should appear in a separate section just after the conclusions. ☒

All abbreviations, in both the abstract and main body of document, are defined once only, the first time they appear in the text. (N.B. The Abstract is treated as an independent text, where references are given in full and abbreviations and symbols, if used, are properly defined.) ☒

Figures – if there are multi-parts to a figures each part is labelled (a) (b) (c) etc. and the labels defined in the figure caption. ☒

Figures – Colour can be used for the on-line version. Figures are reproduced in black and white in the printed journal and must therefore be readable in both colour and black & white. (N.B. charges apply for production of colour figures in the printed journal) ☒

Appendices – should appear before the list of references and labelled A, B, C, (please see GFA for further information regarding equations, figures and tables in the appendices. ☒

Copyright – material reproduced from other publications (e.g. Tables, Figures), source is acknowledged. ☒

List of changes to the manuscript

Lists of the revisions made to the manuscript.

- Page 3, line 8. Spelling mistakes are corrected and amended as "deterministic and indeterministic".
- Page 3, line 9. Spelling mistakes are corrected and amended as "response".
- Page 3, line 14. Spelling mistakes are corrected and amended as "propagation".
- Page 3, line 21. Spelling mistakes are corrected and amended as "response" and "propagation".
- Page 4, line 2. Spelling mistakes are corrected and amended as "separates".
- Page 4, line 5. Spelling mistakes are corrected and amended as "transfer".
- Page 4, line 12. Spelling mistakes are corrected and amended as "important".
- Page 6, line 4. Spelling mistakes are corrected and amended as "sinusoidal".
- Page 10, line 7 from the bottom. Amend "figure" to its abbreviation "Fig.".
- Page 10, line 2 from the bottom. Spelling mistakes are corrected and amended as "uncertainties".
- Page 11, line 8. Amend "figure" to its abbreviation "Fig.".
- Page 11, line 7 from the bottom. Spelling mistakes are corrected and amended as "specifically".
- Page 13, line 2 from the bottom. Spelling mistakes are corrected and amended as "nonlinearity".

CRediT author statement

Fiorenzo Fazzolari: Conceptualization, Methodology;

Fiorenzo Fazzolari, Puxue Tan: Software, Validation;

Puxue Tan: Data curation;

Fiorenzo Fazzolari, Puxue Tan: Writing- Original draft preparation.

Fiorenzo Fazzolari, Puxue Tan: Visualization, Investigation.

Fiorenzo Fazzolari: Supervision;

Fiorenzo Fazzolari, Puxue Tan: Writing- Reviewing and Editing.

*Declaration of Interest Statement

Conflict of interest

The authors declare that there is no conflict of interest regarding the publication of this article.